Polymer Diffusion in Molten Poly(propylene oxide)

Barton A. Smith*

IBM Research Laboratory, San Jose, California 95193

Edward T. Samulski and Li-Ping Yu

Chemistry Department, University of Connecticut, Storrs, Connecticut 06268

Mitchell A. Winnik

Erindale College and Lash Miller Laboratories, Department of Chemistry, University of Toronto, Toronto, Canada M5S 1A1. *Received January 30, 1985*

ABSTRACT: Measurements of the translational diffusion coefficients of poly(propylene oxide) molecules in the melt as a function of molecular weight just above the critical molecular weight for entanglement indicate that constraint release is a significant mechanism for diffusion. Diffusion coefficients of labeled polymer chains in molten poly(propylene oxide) have been measured by fluorescence redistribution after pattern photobleaching both below and above the critical molecular weight for entanglement. Labeled poly(propylene oxide) was synthesized with exactly one fluorophore per molecule. The diffusion coefficients of labeled chains were found to depend upon the length of solvent chains for solvent molecular weights up to four times the critical molecular weight for entanglement.

Introduction

The tube model for the motion of entangled polymer chains[1] and the reptation theory[2] are at present the best models for describing the dynamics of entangled polymer systems. These models allow us to understand in many respects the behavior of polymer melts and concentrated solutions. In the reptation model, the motion of a polymer chain is limited to effective one-dimensional diffusion along a path determined by a set of fixed entanglement points. Theoretical arguments have been made that imply that this model should be an accurate description of polymer self-diffusion in the melt, for chains of sufficient molecular weight.[3] Initial experimental results in solutions[4] and in melts[5,6] have provided evidence that reptation is indeed the dominant mode of motion of entangled polymer chains. However, the well-known discrepancy between the theoretical prediction and the experimental dependence of melt viscosity upon molecular weight and our preliminary findings on the molecular weight dependence of diffusion rate[7] lead us to believe that a more generalized model may be necessary for the complete description of the motion of entangled polymer chains.[8]

In this study, we have measured the rate of diffusion for polymer molecules in the melt in order to investigate possible limitations to the application of reptation theory. In particular, we have measured the diffusion of molecules of moderate molecular weight, just above the critical molecular weight for entanglement. The results are discussed in terms of the observed deviations from the theoretical predictions.

Diffusion Measurements

Fluorescence redistribution after pattern photobleaching (FRAPP) is a method for measuring the translational diffusion coefficients of dye-labeled molecules or particles.[9-11] The technique relies on the availability of fluorescent dyes that can be irreversibly photochemically bleached. Gradients in the concentration of the fluorescent dye are established by exposing portions of the sample to intense light. The diffusion coefficient of the fluorescent species is deduced from the rate at which these concentration gradients decay. The choice of a periodic pattern of bleaching illumination simplifies the data analysis.

For the present experiments, the polymer melt samples were contained in fused-silica cuvettes having dimensions $X = 1$ cm, $Y = 3$ cm, and $Z = 100$ μm. Samples were illuminated both for photobleaching and for subsequent observation of fluorescence by the same periodic intensity pattern. This pattern was produced by the intersection of two coherent beams of light that traversed the sample along the z direction. The light intensity in the sample varied sinusoidally in the x direction and was constant in the y and z directions. The 500-μm-diameter beams were coincident through the thickness of the sample. The light source was an argon ion laser with intracavity etalon producing 0.5 W of output at 488 nm. Total power incident on the sample for photobleaching was 0.2 W. The power was reduced for fluorescence observation by a special modulator to 1 μW or less.[9] The pitch or repeat period of the pattern was varied within the range 4–20 μm by changing the angle of intersection of the beams.

The experimental sequence, which was controlled by an IBM Series/1 computer, was (1) observation of initial fluorescence intensity, (2) photobleaching, and (3) observation of fluorescence intensity as a function of time. The low excitation intensity used for fluorescence observation produced no measurable photobleaching. Duration of the bleaching exposure ranged from 0.2 to 1.0 s and produced reductions in observed intensity of from 25% to 75%.

Interpretation of the diffusion measurement data follows from the solution of the diffusion equation for one dimension with periodic boundary conditions.[9] Since the observation pattern is sinusoidal, only a single Fourier component of the spatial distribution of the fluorophore contributes to the time dependence of the fluorescence intensity. The observed intensity as a function of time after photobleaching is described by

$$I(t) \propto 1 - Ae^{-Da^2t} \tag{1}$$

The constant A is determined by the pattern contrast and extent of bleaching, t is the time, and a is the spatial frequency of the periodic pattern, defined by $a = 2\pi/p$, where p is the pitch of the pattern. The diffusion coefficient is deduced from a least-squares fit of a single-exponential function to the data. Figure 1 shows some typical experimental data.

The above analysis assumes that the motion of the fluorescent molecules can be described by a single diffusion coefficient. This assumption is not strictly true for a polydisperse sample. However, the molecular weight distributions of our labeled samples are sufficiently narrow that a single-exponential curve fits the data quite well. Thus the assumption is valid for our purposes. Two measures have been taken to minimize any small systematic error in the data interpretation due to polydispersity. Since each molecule contains a single fluorophore, the number-average molecular weight for each fraction has been used in analyzing the dependence of the diffusion coefficient on molecular weight of the labeled molecules. In all measurements, the fluorescence intensity after photobleaching was observed for about three times the exponential decay constant of the signal. This method removes any bias that might be introduced by observing the slowly diffusing samples for only the initial part of the decay but observing the

0024-9297/85/2218-1901$01.50/0

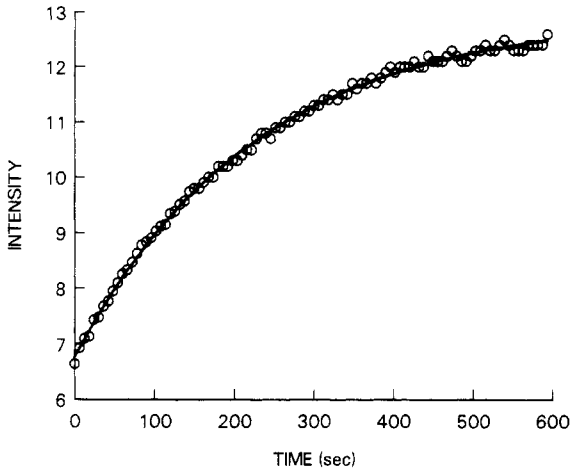

Figure 1. Typical data from FRAPP measurement: fluorescence intensity (each unit represents 10^4 photon counts/s) as a function of time. The circles represent individual 1-s observations of intensity at 6-s intervals. The solid curve represents the best fit of a single-exponential function to the data. The stripe pattern period was 15.6 μm, and the recovery time constant was 227 s. Thus $D = 2.7 \times 10^{-10}$ cm^2 sec^{-1}. M_n of the labeled molecules was 33 600. M_w of the solvent was 12 400. The 100-μm-thick sample had an absorbance of 0.001 at 488 nm. The fluorescence was reduced to 26% of its initial value during the 250-ms bleach and recovered to 50% of the initial value during observation.

rapidly diffusing samples for a relatively longer time.

The values for diffusion coefficients reported here represent the mean of at least 10 measurements on each sample. The sample standard deviation about the mean was typically 2–5%. A series of preliminary experiments showed that the measured diffusion coefficients did not depend upon bleaching beam intensity or duration, observation intensity, the pitch of the pattern, age of the sample (up to 1 year), or prior photobleaching of the same portion of the sample. In addition, uniformly bleached samples (no pattern) showed no recovery of the fluorescence intensity over the maximum time scale of these measurements.

Materials

All of the diffusion experiments reported herein were made on molten poly(propylene oxide) (PPO). The samples were dilute solutions of fluorescent-dye-labeled PPO in neat PPO. The labeled material was produced by the zinc hexacyanocobaltate catalyzed polymerization of propylene oxide, initiated by the dye 4-[bis(2-hydroxyethyl)amino]-7-nitrobenzofurazan.[12] The target molecular weight was achieved by controlling the molar ratio of propylene oxide to initiator. Typically 5 g of propylene oxide (in 15 mL of dry THF with 0.005 g of catalyst and the initiator) was polymerized for 24 h at 75 °C under argon in a thick-walled glass bottle fitted with a corrugated cap having a butyl rubber liner. The solvent was removed by low-pressure distillation and the labeled polymer was dried in vacuo at 70 °C for 24 h.[13]

The initiator dye was made by the reaction of 4-chloro-7-nitrobenzofurazan (Aldrich) with diethanolamine. The 4-chloro-7-nitrobenzofurazan (5.0 g) was added to a mixture of diethanolamine (5 mL) in absolute ethanol (250 mL) and stirred at room temperature for 3 h. The resulting red heterogeneous mixture was then warmed to boiling and upon cooling the product separated as red needle-shaped crystals (mp 155.5 °C), which were isolated by suction filtration. Thin-layer chromatographic analysis (silica gel, 95% chloroform, 5% methanol) indicated the product (R_f 0.20) was free of 4-chloro-7-nitrobenzofurazan (R_f 1.00) and other impurities. NMR analysis results were consistent with the expected structure: 90-MHz ^{1}H NMR (CD_6CO) δ 7.40 (s, 2, Ar H), 4.30 (t, 4, CH_2), 4.00 (t, 4, CH_2), 2.72 (d, 2, OH).

Since the initiating dye is bifunctional, the polymerization produces molecules containing exactly one dye group near the center (Figure 2). The labeled polymer was separated by size exclusion chromatography (SEC) into fractions having narrow molecular weight distributions. Molecular weights of these fractions were measured by SEC on μStyragel columns in tetrahydrofuran (THF). A universal calibration curve was established

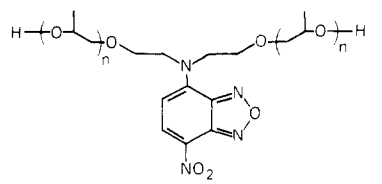

Figure 2. Chemical structure of the dye-labeled polymer.

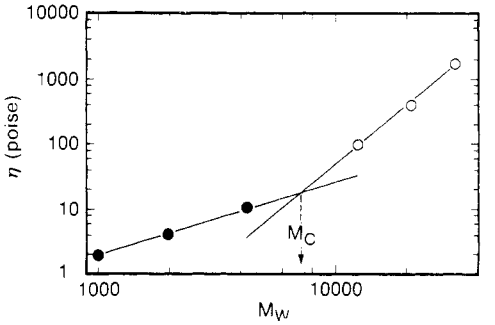

Figure 3. Zero-shear melt viscosity of the solvent polymer samples as a function of molecule weight (measured by light scattering). Measurements were made at 25 °C. Filled circles represent the materials from Polysciences; open circles those from General Tire. The straight lines represent least-squares fits to the data. The intersection of these lines indicates that the critical molecular weight for entanglement, M_c, is around 7000.

Table I
PPO Characterization Results

M_w	M_w/M_n	η(25 °C), P	[η](25 °C, THF), dL/g
1 000	1.1	1.96 ± 0.14	0.033 5
1 960	1.1	3.37 ± 0.13	0.064
4 220	1.2	10.4 ± 0.3	0.086 8
12 400	1.5	98 ± 6	0.229
21 000	1.5	375 ± 15	0.305
32 000	1.6	1 750 ± 50	0.388

for these columns with polystyrene standards. Number-average molecular weights, M_n, were from 500 to 94 000. Polydispersities (M_w/M_n) ranged from 1.06 to 1.13. The SEC molecular weights were reproducible to within 5%. It is difficult to estimate the accuracy of these values since some systematic error is likely to be present in the calibration.

Six lots of unlabeled PPO were used as the solvents in these experiments. Three lower molecular weight materials were purchased from Polysciences, and three higher M_w samples were a gift from General Tire and Rubber Co. Weight-average molecular weights, M_w, were measured by low-angle light scattering. Molecular weight distributions (and M_n) were measured by SEC as above. Zero-shear melt viscosities and intrinsic viscosities were measured for these six solvent samples. Intrinsic viscosities were measured at 25 °C in THF in an Ubbelohde viscometer. Flow times were greater than 100 s and were measured to a precision of 0.2 s. Each polymer sample was measured at four concentrations. Intrinsic viscosity values were consistent with published data.[14] The melt viscosities of the PPO solvents were determined with a hybridization of a cone-and-plate viscometer and a coaxial-cylinder viscometer with a mechanical spectrometer (Rheometrics conicylindrical viscometer). Extrapolated values of the viscosity determined over a range of shear rates (0.001–1 rad/s) at 25 °C were used to calculate the zero-shear viscosity. Table I summarizes these characterization data. The melt viscosity data (Figure 3) indicate that the critical molecular weight for entanglement, M_c, is approximately 7000. This value agrees to within the experimental error with the value of 6000 cited by Van Krevelen.[15] Three of the solvent polymer samples lie below M_c and three lie above M_c in molecular weight.

The samples were prepared for diffusion measurements by adding the labeled polymer in dichloromethane solution to the solvent polymer and then allowing the dichloromethane to evaporate under vacuum at 50 °C. The concentration of the

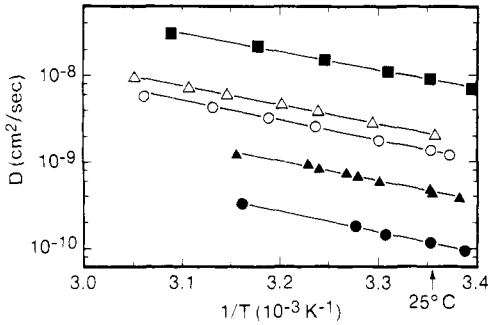

Figure 4. Temperature dependence of polymer melt diffusion coefficients. Straight lines are least-squares fits to the data. Molecular weights of the labeled polymer and solvent polymer in each sample and the apparent activation energies (kcal/mol) were as follows: filled squares, $M_{n,l}$ = 2400, $M_{w,s}$ = 32 000, E_a = 10.2; open triangles, $M_{n,l}$ = 16 800, $M_{w,s}$ = 4200, E_a = 10.0; open circles, $M_{n,l}$ = 92 300, $M_{w,s}$ = 2000, E_a = 10.0; filled triangles, $M_{n,l}$ = 16 800, $M_{w,s}$ = 32 000, E_a = 10.4; filled circles, $M_{n,l}$ = 33 600, $M_{w,s}$ = 32 000, E_a = 10.7.

fluorescent dye in the samples was on the order of 10^{-4} M, resulting in labeled polymer concentrations of from 0.02% to 0.1% by weight. No dependence of D on label concentration was observed in this range. These samples had an absorbance of 0.5 cm^{-1} at 488 nm.

The use of labels to study transport requires us to ask whether the label affects the diffusion coefficients. We have minimized these possible effects in two ways. First, only a single dye molecule is present in each polymer chain. Second, the molecular weights of the labeled chains were measured by size exclusion chromatography. Thus the hydrodynamic volume of the dye group has been included in the M_n values used in the data analysis. While a small effect may be present, it will not alter the trends in the data on which we base our conclusions.

Results

Figure 4 is an Arrhenius plot showing the temperature dependence of the diffusion coefficients for five of the polymer/polymer solutions. The activation energy for diffusion is roughly independent of the size of diffusant or solvent molecules within this range of molecular weights, as previously observed in polyethylene.[16] These data are consistent with the idea that for polymer melts well above T_g, the primary effect of changing temperature upon D lies in its effect upon the monomer friction coefficient, which is independent of molecular weight for large molecules.[17] (T_g for poly(propylene oxide) is 198 K.[18]) This idea supports the use of topological models for the dynamics of entangled chains. The microscopic details of the dynamics which are absent from these models can be assumed to be independent of the state of entanglement.

Figure 5 shows how the diffusion coefficients of the labeled molecules depend upon their molecular weight. Each curve represents a series of labeled molecules of varying M_n dissolved in a particular host polymer. Two types of behavior are seen, depending upon whether the solvent polymer has a molecular weight M_w greater than or less than the critical molecular weight for entanglement, M_c. When necessary for clarity, we will denote the number-average molecular weights of the fluorescent labeled polymer samples by M_n, and the weight-average molecular weights of the solvent (host) polymer samples by $M_{w,s}$.

In solvents with $M_{w,s} < M_c$, the diffusion coefficients of the labeled molecules exhibit a single power-law dependence on their molecular weights over the entire range 500 $< M_{n,l} <$ 94 000. For $M_{w,s}$ = 1960, $D \propto M_{n,l}^{-0.6}$. For $M_{w,s}$ = 4220, $D \propto M_{n,l}^{-0.75}$. No effects of entanglement are seen, since the labeled molecules are present in low concentrations (the dilute regime). Under these conditions, the exponents for diffusion depend primarily upon the degree

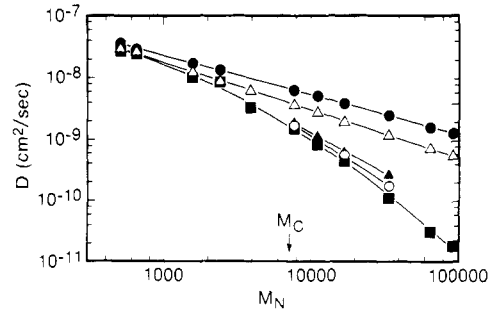

Figure 5. Diffusion coefficient as a function of the number-average molecular weight of the labeled molecules for five different solvent molecular weights. All data are for polymer melt samples at 25 °C. Molecular weights of the solvent polymers were as follows: filled circles, $M_{w,s}$ = 2000; open triangles, $M_{w,s}$ = 4200; filled triangles, $M_{w,s}$ = 12 400; open circles, $M_{w,s}$ = 21 000; filled squares, $M_{w,s}$ = 32 000.

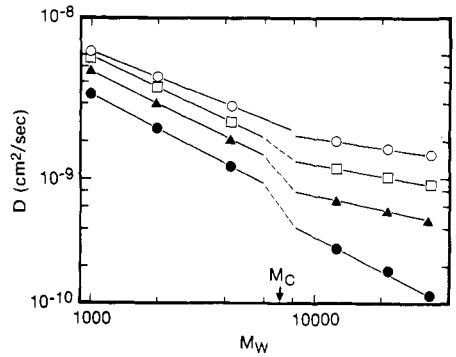

Figure 6. Diffusion coefficient as a function of solvent molecular weight for four different labeled polymer fractions. Molecular weights of the labeled molecules were as follows: open circles, $M_{n,l}$ = 7600; open squares, $M_{n,l}$ = 11 000; filled triangles, $M_{n,l}$ = 17 000; filled circles, $M_{n,l}$ = 33 600.

to which hydrodynamic interactions between segments of the chain contribute to its friction coefficient. For a monomeric Θ solvent, we expect the exponent to be −0.5. When hydrodynamic interactions are completely screened, we expect an exponent of −1.0.[19,20] These data show a behavior intermediate between these two limits, with hydrodynamic interaction decreasing as the molecular weight of the solvent increases.

In solvents with $M_{w,s} > M_c$, no simple power-law dependence is seen, but the effects of entanglements are clearly present. The slope of log D vs. log $M_{n,l}$ decreases continuously as $M_{n,l}$ increases. For $M_{w,s}$ = 32 000, the slope reaches a value of −1.9 for the highest molecular weight of labeled molecules, M_n = 94 000. Thus the slope approaches, but does not reach, the value −2.0, which is predicted by the reptation model. In other words, the strongest dependence of D upon labeled molecular weight for these samples is $D \propto M_{n,l}^{-1.9}$, even in a solvent that has M_w four times M_c.

Figure 6 shows how the diffusion coefficient of a labeled molecule depends upon the molecular weight of the solvent (host) polymer. Data are shown for four molecular weights of labeled molecules. The shortest of these test chains, $M_{n,l}$ = 7600, have a molecular weight near the viscosity-determined M_c. The longest, $M_{n,l}$ = 33 600, have a molecular weight just above that of our highest molecular weight solvent. We will first discuss the data for diffusion in the lower molecular weight solvents: $M_{w,s} < M_c$. In this range, the diffusion coefficient depends strongly on the molecular weight of the solvent, and the magnitude of the dependence increases as the molecular weight of the labeled chains increases. For labeled M_n = 7600, $D \propto M_{w,s}^{-0.7}$; for

labeled M_n = 11 000, $D \propto M_{w,s}^{-0.86}$; for labeled M_n = 17 000, $D \propto M_{w,s}^{-0.87}$; and for labeled M_n = 33 600, $D \propto M_{w,s}^{-0.93}$. For a polymer in monomeric solvents, we would expect the polymer diffusion coefficient to be inversely proportional to the solvent viscosity. In this series of polymeric solvents, additional factors are introduced by the dependences of both the hydrodynamic screening length[19] and the hydrodynamic radii of the diffusing molecules[21] upon the molecular weight of the solvent. Therefore, the results approach $D \propto \eta^{-1}$ only as the diffusing molecules become much longer than the solvent molecules.

We will next discuss diffusion in the entangled solvents. For the shorter test chains, the slope of D vs. $M_{w,s}$ is sensitive to the onset of the entangled state of the solvent. This onset occurs over roughly the same molecular weight range as does the change in the slope of melt viscosity vs. $M_{w,s}$. Thus for solvent M_w greater than M_c, it appears that reptation is the dominant mechanism for diffusion. However, the diffusion coefficient does not become totally independent of solvent molecular weight above M_c, as would be the case if reptation were the only diffusion mechanism. For labeled M_n = 7600, $D \propto M_{w,s}^{-0.25}$. As the length of the test chains increases, the effect of the solvent molecular weight on D becomes stronger. For labeled M_n = 11 000, $D \propto M_{w,s}^{-0.34}$; for labeled M_n = 17 000, $D \propto M_{w,s}^{-0.40}$; and for labeled M_n = 33 600, $D \propto M_{w,s}^{-0.93}$. Thus the reptation model fails to describe accurately diffusion for molecular weights just above M_c when the diffusing molecules and solvent molecules are of comparable length. We conclude that the constraint-release mechanism contributes significantly to diffusion in this regime. The term "constraint release" refers to the relaxation of the entanglement constraints through motions of the surrounding chains rather than through reptation of the labeled chain. This mechanism has also been referred to as "tube renewal".[3] Léger et al. have also observed a small but measurable dependence of D on the molecular weight of surrounding chains (ref 4, Figure 7).

Another prominent feature of these data is the sharp decrease in diffusion coefficient as the solvent molecular weight passes through M_c. We were initially concerned that the different methods of preparation for the two sets of samples might lead to tacticity differences or other chemical differences that could affect the absolute values of the diffusion coefficients. We now discount the importance of matrix effects other than molecular weight. Our intrinsic viscosity and melt viscosity measurements indicate no fundamental differences between the two sets of solvent samples. More important, the virtually identical activation energies for diffusion shown in Figure 4 indicate similar interaction energies for the solute chains with both sets of solvents. Finally, the self-diffusion coefficients (Figure 7) measured for these samples vary smoothly through this molecular weight range.

Theory suggests that a break in this regime is to be expected. Constraint release is predicted to be the dominant diffusion mechanism for long chains in a matrix just above M_c,[22] leading to a sharp decrease in solute chain diffusion with increasing solvent molecular weight. Indeed this behavior has been observed in other systems.[23,25]

We expect that D would become independent of solvent M_w for sufficiently high solvent molecular weights. Such behavior has been observed.[23-25] It is unfortunate that we were unable to obtain higher M_w samples for this study.

Discussion

Due to the dependence of the diffusion coefficient of the labeled molecules upon the molecular weight of the solvent above M_c, we have concluded that the reptation mechanism does not provide a complete description of diffusion in this molecular weight range. This conclusion would seem at first to be in conflict with previous reports, in which the self-diffusion coefficient was seen to obey the reptation prediction, $D \propto M^{-2}$, even for molecular weights just above M_c.[4] However, our data on these samples are consistent with those previous results. Figure 7 shows the self-diffusion coefficient as a function of molecular weight. Within a reasonable approximation, $D \propto M^{-2}$ above M_c. The observed molecular weight dependence of the self-diffusion coefficient appears to be a combination of dependence upon both diffusant and solvent molecular weights (Figures 5 and 6). Thus the measurement of self-diffusion may not be as rigorous a test of the theory as is the independent variation of diffusant and solvent molecular weights.

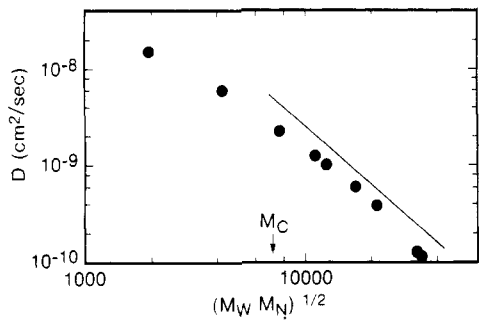

Figure 7. Self-diffusion coefficient of PPO in the melt at 25 °C as a function of molecular weight. The data points are interpolated values from curves of D vs. molecular weight like those shown in Figures 5 and 6. Each value corresponds to the point on the curve at which $M_{n,l} = M_{w,s}$. The straight line is drawn with a slope of −2 for illustration purposes.

Dr. William Graessley has pointed out to us that a direct comparison can be made between our results for self-diffusion and the prediction of the Doi–Edwards theory[26] (assuming pure reptation). We begin with Graessley's expression for D (ref 26, eq 19) and make a substitution for the plateau modulus, G^0_N, using $M_e = \rho RT/G^0_N$ and estimating $M_e \sim M_c/2$

$$D = \left(\frac{M_c}{M}\right)^2\left(\frac{1}{270}\right)\left(\frac{\rho RT}{\eta_{M_c}}\right)\frac{\langle R^2\rangle}{M} \qquad (2)$$

$R = 8.31 \times 10^7$ erg K^{-1} mol^{-1} is the gas constant, T = 298 K is the temperature, ρ = 1.0 g/mL is the density, η_{M_c} = 20 P is the zero-shear melt viscosity at the critical molecular weight for entanglement, and $\langle R^2\rangle/M = 5.6 \times 10^{-17}$ cm^2 mol g^{-1} is the mean squared end-to-end distance per molecular weight unit.[27]

Our measured values for self-diffusion for $M > M_c$ (see Figure 7) are roughly 1 order of magnitude higher than the values calculated from eq 2. For example, for M = 33 600, where $M = 4.8 \times M_c$, the predicted value for D is 1.1×10^{-11} cm^2/s. The measured value is $D = 1.13 \times 10^{-10}$ cm^2/s. In other words, the measured values are 10 times faster than that predicted by eq 2. This is further evidence that for this molecular weight, the diffusion mechanism is not limited to reptation.

Reptation is a simple model full of interesting physical insights into the behavior of molecules. One does not expect the reptation model to describe in detail all of the different facets of polymer motion in concentration solutions and melts. such a complete description is important; further efforts in this direction are clearly warranted.

Acknowledgment. We thank Dr. Patricia M. Cotts of IBM Research for assistance in molecular weight determinations, Dr. Robert J. Herold of the General Tire and

Rubber Co., R&D Division for the catalyst and high molecular weight PPO samples, and Dr. Leo Kadehjian for synthesis of the initiator dye. We also thank Dr. G. Ronca and Dr. G. Hadziioannou of IBM Research for helpful discussions.

References and Notes

(1) Edwards, S. F. In "Molecular Fluids"; Balian, R., Weill, G., Eds.; Gordon and Breach: London, 1976; pp 151–208.
(2) de Gennes, P.-G. "Scaling Concepts in Polymer Physics"; Cornell University Press: Ithaca, NY, 1979.
(3) Daoud, M.; de Gennes, P.-G. *J. Polym. Sci., Polym. Phys. Ed.* **1979**, *17*, 1971–1981.
(4) Léger, L.; Hervet, H.; Rondelez, F. *Macromolecules* **1981**, *14*, 1732.
(5) Klein, J. *Nature (London)* **1978**, *271*, 143–145.
(6) Klein, J.; Briscoe, B. J. *Proc. R. Soc. London, A* **1979**, *365*, 53–73.
(7) Smith, B. A.; Samulski, E. T.; Yu, L.-P.; Winnik, M. A. *Phys. Rev. Lett.* **1984**, *52*, 45–48.
(8) Wendel, H.; Noolandi, J. *Macromolecules* **1982**, *15*, 1318–1320.
(9) Smith, B. A. *Macromolecules* **1982**, *15*, 469–472.
(10) Smith, B. A.; McConnell, H. M. *Proc. Natl. Acad. Sci. U.S.A.* **1978**, *75*, 2759.
(11) Smith, L. M.; Smith, B. A.; McConnell, H. M. *Biochemistry* **1979**, *18*, 2256.
(12) Livigni, R. A.; Herold, R. J.; Eliner, O. C., Aggarwal, S. L. *ACS Symp. Ser.* **1975**, *No. 6*, 20.
(13) Yu, L.-P. Ph.D. Dissertation, University of Connecticut, 1984.
(14) Scholtan, V. W.; Lie, S. Y. *Makromol. Chem.* **1967**, *108*, 104.
(15) Van Krevelen, D. W. "Properties of Polymers", 2nd ed.; Elsevier: Amsterdam, 1976; p 339.
(16) Klein, J.; Briscoe, B. J. *Proc. R. Soc. London, A* **1979**, *365*, 53.
(17) Ferry, J. D. "Viscoelastic Properties of Polymers", 2nd ed.; Wiley: New York, 1970.
(18) Brandrup, J., Immergut, E. H., Eds. "Polymer Handbook", 2nd ed.; Wiley: New York, 1975; p III–158.
(19) Kirkwood, J. G.; Riseman, J. *J. Chem. Phys.* **1948**, *16*, 565–573.
(20) Debye, P.; Bueche, A. M. *J. Chem. Phys.* **1948**, *16*, 573–579.
(21) Flory, P. *J. Chem. Phys.* **1949**, *17*, 303–310.
(22) Graessley, W. W. *Adv. Polym. Sci.* **1982**, *47*, 67–117.
(23) Tanner, J. E. *Macromolecules* **1971**, *4*, 748–750.
(24) Klein, J. *Macromolecules* **1981**, *14*, 460–461.
(25) Green, P. F.; Mills, P. J.; Palmstrom, C. J.; Mayer, J. W.; Kramer, E. J. *Phys. Rev. Lett.* **1984**, *53*, 2145–2148.
(26) Graessley, W. W. *J. Polym. Sci., Polym. Phys. Ed.* **1980**, *18*, 27–34.
(27) Brandrup, J., Immergut, E. H., Eds. "Polymer Handbook", 2nd ed.; Wiley: New York, 1975; p IV–45.

Normal Vibrational Analysis of Benzanilide. A Model for Poly(*p*-phenylene terephthalamide)

P. K. Kim and S. L. Hsu*

Polymer Science and Engineering Department, University of Massachusetts, Amherst, Massachusetts 01003

H. Ishida

Department of Macromolecular Science, Case Western Reserve University, Cleveland, Ohio 44106. *Received January 16, 1985*

ABSTRACT: Vibrational analysis has been carried out for benzanilide, a model compound of poly(*p*-phenylene terephthalamide). The normal coordinate analysis has been carried out by using a set of nonredundant symmetry coordinates to overcome the difficulties in defining the appropriate force field. Satisfactory assignments were made for the infrared and Raman spectra obtained.

Introduction

A significant number of studies have been directed toward understanding the structure–property relationships of high-modulus/high-strength fibers or films of rigid-rod polymers such as poly(*p*-phenylene terephthalamide) (PPTA).[1,2] The structure of this polymer is shown schematically below.

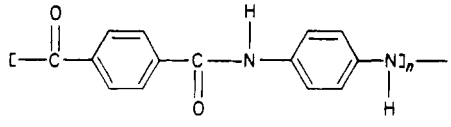

The molecular basis of the mechanical properties obtained for PPTA is largely due to the inherent chain stiffness and the high molecular structural order achieved during processing. For PPTA-like polymers, the formation of fibers or films involves several steps: (1) dissolution into strong acids such as 100% sulfuric acid with sufficiently high concentration to form an anisotropic liquid crystalline state, (2) extrusion of this anisotropic solution into a coagulating bath, (3) neutralization and washing of the fibers and films, and (4) post-processing heat treatment.[3,4]

Therefore, information about the molecular structure in solution, polymer–solvent interaction, chain segment orientation, and the nature, specificity, or magnitude of the intermolecular interactions is important from both the practical and fundamental viewpoints. When bands are

Table I
Structural Parameters of a Proposed Geometry of Benzanilide

length, Å		valence angle, deg		dihedral angle, deg	
C–C	1.397	<(CCC)	120	τ(CCCC)	180
C–H	1.084	<(CCH)	120	τ(CCCH)	0
N–H	1.084	<(CCN)	120	$\tau(C_4C_5HN)$	30
C–N	1.42	<(CCC′)	120	$\tau(C_4C_5NH)$	210
N–C′	1.34	<(CNH)	120	τ(HNC′O)	0
C′–O	1.24	<(CNC′)	125	$\tau(NC'C_{16}C_{21})$	210
C′–C[a]	1.47	<(CC′O)	120	$\tau(OC'C_{16}C_{21})$	30
		<(NC′C)	117		

[a] C′ = carbonyl carbon; C = ring carbon.

* To whom correspondence should be addressed.

0024-9297/85/2218-1905$01.50/0